2022 IEEE 61st Conference on Decision and Control (CDC)
December 6-9, 2022. Cancún, Mexico

NMR Pulse Design using Moment Dynamical Systems

Xin Ning, André Luiz P. de Lima, and Jr-Shin Li

2022 IEEE 61st Conference on Decision and Control (CDC) | 978-1-6654-6761-2/22/$31.00 ©2022 IEEE | DOI: 10.1109/CDC51059.2022.9992480

Abstract— **We investigate pulse design problems arising in diverse applications in quantum science and technology. In modern approaches, pulse design is cast as an ensemble control problem involving the control of a continuum of nuclear spin systems, which, however, is typically challenging to solve. In this paper, we present a new pulse design paradigm by introducing moment representations of the spin ensemble system and transforming the ensemble control problem associated to pulse design to a moment control problem. We show that feasible and optimal pulses can be effectively designed using the moment system with performance guarantees across the entire ensemble. We also illustrate the versatility and robustness of our moment-based approach by designing uniform and selective pulses essential to enable prominent applications in magnetic resonance.**

I. Introduction

Nuclear Magnetic Resonance (NMR) spectroscopy and imaging (MRI) are precise and non-invasive techniques for analyzing and reconstructing molecular compositions and images. They have facilitated advancements in various research fields, such as medical diagnoses [1], material science [2], physics and biophysics [3], brain science, and fluid dynamics [4], [5]. The key to the development of NMR methodologies is the study of Bloch equations that model the time-evolution of the bulk magnetization of a spin ensemble immersed in a static magnetic field and controlled by external radio-frequency (rf) fields [6], [7]. In real applications, engineered rf fields of a certain duration is applied to align the magnetization vector with a desired target on the Bloch sphere.

Within this context, the pulse design problem entailing the construction of applied rf fields to consistently manipulate the spin population of enormous scale is challenging. Not only we have the intrinsic nonlinearity of Bloch equations, but also inhomogeneity induced by chemical shift, magnetic field inhomogeneity and magnetic susceptibility variations differentiate spin dynamics [7]. Hence, attempting to deal with these divergences individually is intractable, as the required calculations are expensive and the control dynamics are in dire need for robustness.

Commonly adopted approaches for pulse design in NMR and MRI either rely on approximations of the underlying Bloch equations or cater to specific magnetization profiles under different inhomogeneity considerations. For instance, rf fields taking the form of hard pulse, SINC pulse [8] and SLR pulses [9] are obtained from time-domain Fourier transformation of the target spectral magnetization profile by limiting the flip angle to small values. Otherwise, a so-called adiabatic pulse can be applied, requiring additional constraints [7]. Other methods that integrate optimal control theory [10], [11] or Fourier series analysis [12] have also been developed for pulse design. Noticeably, recent works have achieved promising results by treating Bloch systems subjected to inhomogeneity as an ensemble dynamics [13], [14], which consists of a continuum of dynamical systems and a single broadcasting control signal.

In virtue of the ensemble system description, the pulse design problem is naturally cast as an ensemble control problem. Our work fits in this setting and aims to seek for a unified approach for pulse design problem that applies to disparate tasks with computational efficiency. To resolve this, recent works of moment dynamics from our lab and other colleagues [15]–[17] granted the shift from the study of parameterized ensemble system to its nonparameterized counterparts evolving within a Hilbert space. One benefit of this transformation is that we can leverage the theoretical results for dynamical systems within a Hilbert space setting to help analyze ensemble controllability [18]–[20]. Another advantage is that the ensemble control problem becomes manageable via truncating the moment dynamics as a finite dimensional system, thus allowing more flexibility in constructing the control.

In this paper, we extend the idea of moment dynamical system to ensemble dynamics of bilinear form, and construct feasible controls based on a truncated moment system. The proposed method not only enables us to design pulses that achieve different magnetization patterns, but also expand the possibilities for diverse pulse shapes. In particular, this paper is organized as follows: The Bloch ensemble dynamics and its corresponding moment dynamics are derived in section II, followed by a pulse design approach established from a truncated version of the obtained moment dynamics in section III, where we also conduct analysis of error terms. The simulation results for different final profiles are demonstrated in section IV and followed by conclusions in section V.

II. Spin Ensemble System and its Moment System

A. Spin Ensemble Dynamics and Bloch Systems

The Bloch equations describe the time-evolution of the bulk magnetization of a spin ensemble under a static magnetic field. The magnetization can be perturbed by external rf fields, which are referred to as pulse sequences. In the regime where the duration of the applied pulses is shorter

This work was supported in part by the National Science Foundation under the awards ECCS-1810202 and CMMI-1933976, and by the Air Force Office of Scientific Research under the award FA9550-21-1-0335.

X. Ning, A.L.P. de Lima, and J.-S. Li are with the Department of Electrical and Systems Engineering, Washington University in St. Louis, St. Louis, MO 63130, USA xin.ning@wustl.edu, a.delima@wustl.edu, jsli@wustl.edu

than the relaxation times [6], the Bloch equations follow the dynamic law,

$$\begin{aligned}\dot{M} &= \begin{pmatrix} 0 & -\omega_0 & u_1(t) \\ \omega_0 & 0 & -u_2(t) \\ -u_1(t) & u_2(t) & 0 \end{pmatrix} M \\ &\doteq \big[\omega_0\Omega_z + u_1(t)\Omega_y + u_2(t)\Omega_x\big]M, \end{aligned} \tag{1}$$

where $M = (M_x, M_y, M_z)'$ denotes the bulk magnetization, ω_0 is the Larmor frequency detuning of the spins in the rotational frame, $u_1(t)$ and $u_2(t)$ are the rf pulses (controls) applied along the y- and the x-axis, respectively, and Ω_x, Ω_y, and Ω_z are the generators of rotation around the respective axis. The system (1) is a dimensionless description and the corresponding physical terms are explained in Appendix A. A typical goal in NMR applications is to design an rf-pulse $u(t) = (u_1(t), u_2(t))'$ of duration T that excites the Bloch system from the equilibrium state $M(0) = (0, 0, 1)'$ to an excited state, e.g., $M(T) = (1, 0, 0)'$.

In practice, however, heterogeneities arise across the spin ensemble due to the chemical shifts and inhomogeneous intensity of the applied rf fields (rf-inhomogeneity). Therefore, the system parameters in (1) exhibit variations, which gives rise to the consideration of a parameterized Bloch system of the form

$$\frac{d}{dt}M(t,\omega,\beta) = \big[\omega\Omega_z + \beta u_1\Omega_y + \beta u_2\Omega_x\big]M(t,\omega,\beta), \tag{2}$$

where $\omega \in [-K, K]$ and $\beta \in [1-\delta, 1+\delta]$, $\delta \in (0, 1)$, depict the Larmor dispersion and rf-inhomogeneity, respectively. Furthermore, $M(t, \cdot, \cdot)$ is defined on $L^2([-K, K] \times [1 - \delta, 1 + \delta])$ as in [21]. As a result, pulse design becomes very challenging as one needs to control a parameterized family (an ensemble) of systems in (2) with a common control signal $u(t)$.

In the next section, we will introduce a method of moments that makes the pulse design tractable and systematic by transforming the underlying infinite-dimensional Bloch ensemble system in (2) to a system governed by moment dynamics.

B. Legendre-moments and moment systems

Moment-based methods have been recently proposed to investigate linear ensemble systems [15], [17], which transferred a linear ensemble system defined on the space of L^2 to a moment system defined on the Hilbert space ℓ^2. Although the transformed moment system remains infinite-dimensional, the moment dynamics are independent of the system parameters, e.g., ω and β in (2), this feature, together with the properties of ℓ^2, facilitate the control-theoretic analysis and pulse design based on the use of the truncated moment systems with quantifiable performance guarantees.

Here, we extend the development in [15] to establish a Legendre-moment method for pulse design by introducing the Legendre-moments associated with Bloch ensemble system, defined by

$$m(t) = \int_{-1}^{1} P(\beta) \otimes M(t,\beta)d\beta, \tag{3}$$

where $m(t) = (m_0(t), m_1(t), \dots, m_k(t), \dots)'$ is an infinite sequence of Legendre moments with m_k referred to as the k^{th}-order moment, $P = (P_0(\beta), P_1(\beta), \dots)'$ with $P_k(\beta)$ denoting the normalized Legendre polynomial in β, rescaled to $[-1, 1]$, of order k, and $\otimes$ is the Kronecker product.

To elaborate the ideas of our development, we first consider pulse design to compensate for rf-inhomogeneity, and defer other cases to Appendix B; namely, we consider the Bloch ensemble system in the rotating frame with respect to the Larmor frequency ω_0 in (1),

$$\frac{d}{dt}M(t,\beta) = \big[\beta u_1 B_1 + \beta u_2 B_2\big]M(t,\beta), \tag{4}$$

with $\beta \in [1-\delta, 1+\delta]$, and $B_1 = \Omega_y$, $B_2 = \Omega_x$. By taking the time-derivative of $m(t)$ in (3), we obtain the Legendre-moment system,

$$\dot{m}(t) = \left(\sum_{i=1}^{2} \hat{B}_i u_i\right) m(t), \tag{5}$$

where $\hat{B}_i = \mathcal{C} \otimes B_i$ and $\mathcal{C}$ is the coefficient matrix of the form $\mathcal{C} = \delta\mathcal{C}_0 + \mathcal{I}$ with

$$\mathcal{C}_0 = \begin{pmatrix} 0 & C_1 & & & \\ C_1 & \ddots & \ddots & & \\ & \ddots & 0 & C_k & \\ & & C_k & \ddots & \ddots \\ & & & \ddots & \ddots \end{pmatrix}, k \in \mathbb{Z}^+.$$

The entries C_k are derived using the recursive relation of Legendre polynomials [17] (see Appendix C), and $\mathcal{I}$ denotes the identity matrix of infinite-dimension. Note that $\mathcal{C}$ is a bounded operator since all the entries are uniformly bounded [22], and it is equipped with a banded structure. Therefore, $\hat{B}_i$s are also bounded operators with banded structure.

Thanks to the orthogonality of Legendre polynomials, a nice feature accompanying with the introduced Legendre-moment transformation is an induced isometry between the state of the moment and the Bloch ensemble system in (5) and (2), respectively, i.e.,

$$\|M(t,\cdot) - M_f(\cdot)\|_{L^2} = \|m(t) - m_f\|_{\ell^2}, \tag{6}$$

where $m(t)$ and m_f are the moment sequences corresponding to the ensemble states $M(t, \beta)$ and $M_f(\beta)$, respectively (see Appendix C). The isometry permits the design of pulses by using the Legendre-moment system, through which the performance of pulse design can be theoretically quantified.

III. Pulse Design using truncated moment system

A. Optimal control of truncated moment system

A prominent goal in quantum control applications is to engineer time-varying fields that navigate a spin ensemble from an initial profile, e.g., the equilibrium state $M_0(\beta)$, to a desired excitation profile, $M_f(\beta)$, at a prescribed time $T > 0$. The performance of such control design can be measured by the excitation error, i.e., $\|M_f(\cdot) - M(T, \cdot)\|_{L^2}$. With the moment-based method presented in Section II-B, the design task can be achieved by utilizing the moment system that describes the entire spin ensemble dynamics with moment representations, which are independent of the individual systems in the ensemble. Although the moment system as in (5) defined on ℓ^2 is infinite-dimension, the convergence of the ℓ^2 moment sequence $m(t)$ allows us to design pulses using truncated moment systems and formulate the pulse design as an optimal control problem of the form,

$$\min_{(u_1,u_2)} \quad \|\bar{m}_N(T) - \bar{m}_f\| \tag{7}$$

$$\text{s.t.} \quad \dot{\bar{m}}_N(t) = \left(\sum_{i=1}^{2} \hat{B}_{Ni} u_i\right) \bar{m}_N(t), \tag{8}$$

where N is the truncation order and $\bar{m}_f$ denotes the target state of the truncated moment system. Note that a proper order can be selected so that the truncated moment system as in (8) approximates the moment system sufficiently well. This newly formulated optimal control of a finite-dimensional moment system is the key to effective pulse design, which was arduous to perform through the optimal control of the original Bloch ensemble system in (2). In addition, the above optimal control problem can be solved by various available direct and indirect computational algorithms, such as pseudo-spectral and gradient-based methods [23]–[25].

B. Error analysis

Combining the isometry in (6) and the use of truncated moment systems, we are able to quantify and control the pulse design performance. We first observe that the terminal error in the moment system is bounded by

$$\begin{aligned}&\|m(T) - m_f\| \\ &\leq \|m(T) - \bar{m}_N(T)\| + \|\bar{m}_N(T) - \bar{m}_f\| + \|\bar{m}_f - m_f\|.\end{aligned} \tag{9}$$

Since $\|\bar{m}_f - m_f\|$, i.e., the discrepancy between the desired final state of the moment and the truncated moment system, can be controlled by a suitable choice of the truncation order N, and $\|\bar{m}_N(T) - \bar{m}_f\|$ is optimized by the designed pulse and is 0 if the system in (8) is controllable, the error in (9) can be analyzed by estimating $\|m(T) - \bar{m}_N(T)\|$.

In practice, we may choose a truncation order N such that $\max\{\|\bar{m}_f - m_f\|, \|\bar{m}_0 - m_0\|\} < \epsilon$ for a given tolerance $\epsilon > 0$. By applying piecewise-constant controls, the solutions to the moment and truncated moment systems with the respective initial states m_0 and $\bar{m}_0$ can be expressed by

$$m(T) = S_l(\Delta_t) \circ S_{l-1}(\Delta_t) \circ \ldots \circ S_1(\Delta_t) \circ m_0,$$
$$\bar{m}_N(T) = \bar{S}_l(\Delta_t) \circ \bar{S}_{l-1}(\Delta_t) \circ \ldots \circ \bar{S}_1(\Delta_t) \circ \bar{m}_0,$$

where the time interval $[0, T]$ is partitioned into l subintervals with the time-step Δ_t; $S_k(\Delta_t)$ denotes the exponential propagation under the constant control $(u_1^{t_k}, u_2^{t_k})'$ within subinterval k, and $\circ$ denotes the composition of the propagations, i.e., $S_{k+1} \circ S_k$ denotes the exponential propagation under piece-wise constant controls $(u_1^{t_k}, u_2^{t_k})'$ for subinterval $[(k-1)\Delta_t, k\Delta_t)$, followed by a subsequent piece-wise constant control $(u_1^{t_{k+1}}, u_2^{t_{k+1}})'$ for subinterval $[k\Delta_t, (k+1)\Delta_t)$. Furthermore, $S_k \circ m_{k-1}$ represents the moment state achieved from m_{k-1} by following the evolution of propagation S_k.

By defining $\epsilon_0 = \|m_0 - \bar{m}_0\|$, $\epsilon_1 = \|S_1 \circ m_0 - \bar{S}_1 \circ \bar{m}_0\|$ (To make sense of the subtraction in ϵ_1, we denote $\bar{S}_1 \circ \bar{m}_0$ as its embedding to ℓ^2, where infinite zeros are appended to the finite vector), we have by triangle inequality that $\epsilon_1 \leq \bar{\epsilon}_1 \|m_0\| + \|\bar{S}_1\| \epsilon_0$. The term $\bar{\epsilon}_1 = \|S_1 - \bar{S}_1\|$ under a bounded control input, can be made arbitrarily small as the truncation order $N \to \infty$. This is because S_1 is a bounded operator and $\hat{B}_i$ parameters are equipped with a banded structure [26], [27]. We omit Δ_t from S_1 to further simplify the notations, and obtain the following recursive relation of the error terms,

$$\epsilon_i \leq \bar{\epsilon}_i \|S_{i-1} \circ \ldots \circ S_1 \circ m_0\| + \|\bar{S}_i\| \epsilon_{i-1}, i \geq 2,$$

where $\epsilon_i = \|S_i \circ \ldots \circ S_1 \circ m_0 - \bar{S}_i \circ \ldots \circ \bar{S}_1 \circ \bar{m}_0\|$ and $\bar{\epsilon}_i = \|S_i - \bar{S}_i\|$. Since $\|\bar{S}_i\|$ is bounded and can be made sufficiently small for small interval Δ_t, and $\|S_{i-1} \circ \ldots \circ S_1 \circ m_0\|$ is also bounded, we obtain that

$$\begin{aligned}\epsilon_l \leq &\left(\prod_{i=1}^{l} \|\bar{S}_i\|\right) \epsilon_0 + \bar{\epsilon}_l \|S_{l-1} \circ \ldots \circ S_1 \circ m_0\| \\ &\qquad + \|\bar{S}_l\| \bar{\epsilon}_{l-1} \|S_{l-2} \circ \ldots \circ S_1 \circ m_0\| + \ldots \\ &\qquad + \|\bar{S}_l\| \|\bar{S}_{l-1}\| \ldots \|\bar{S}_2\| \bar{\epsilon}_1 \|m_0\| \\ \leq &\left(\prod_{i=1}^{l} \delta_2^i\right) \epsilon_0 + l\delta_1 \delta_2^{l-1} \|m_0\|,\end{aligned}$$

where we let $\max_i \bar{\epsilon}_i < \delta_1$ and $\max_i(\max(\|S_i\|, \|\bar{S}_i\|)) < \delta_2$. When $l \to \infty$, we arrive at

$$\|m(T) - \bar{m}_N(T)\| \leq \lim_{l \to \infty} \left(\prod_{i=1}^{l} \delta_2^i\right) \epsilon_0 + l\delta_1 \delta_2^{l-1} \|m_0\|,$$

where the upper bound approaches 0 as l increases. Notice that δ_1 appeared in the above inequality measures the precision of representing the infinite-dimensional moment dynamics using the truncated moment system, and it can be made smaller by increasing N. This error analysis offers transparent guidelines for us to quantify and control the pulse design performance. In the next section, we present various pulse design examples to demonstrate the applicability and effectiveness of the developed Legendre-moment method.

IV. Numerical Examples of Pulse Design

The pulse design problem has been formulated as an ensemble control problem involving the Bloch system as in (4), and the objective is to steer the ensemble from an initial state $M(0, \beta) = (0, 0, 1)'$ to a desired excited profile $M_f(\beta)$ at a given time T. In this section, we handle various essential pulses design problems in NMR and quantum optics and manifest the promising capability of the proposed moment-based method in Section III. All of the pulses presented below are obtained by solving the optimal control problem in (7) and (8) by employing an iterative control scheme described in [28]. In particular, we consider the case of 40% rf-inhomogeneity, i.e., $\delta = 0.4$, and a nominal pulse amplitude $A_0 = 20$ kHz. In our simulations, we normalize the parameters with respect to A_0 and set T as the dimensionless time length, namely, the physical time t displayed in the simulation results is computed by multiplying a scale factor $1/(2\pi A_0)$ to the dimensionless time.

A. Uniform Pulse Design

1) Uniform Excitation Pulse in the Presence of RF-Inhomogeneity: Uniform excitation of a spin ensemble is a critical task in high-resolution NMR spectroscopy. The control goal is to excite the spin population from the equilibrium state, $M_0(\beta) = (0, 0, 1)'$ (blue circle in Figure 1) to a final state on the equatorial plane of the Bloch sphere, e.g., $M_f(\beta) = (1, 0, 0)'$ (orange circle in Figure 1). The obtained results for sampled trajectories, distribution of the obtained $M_x(T)$ and the constructed controls are displayed in Figure 1. For this task, we derive the corresponding truncated moment dynamics for the given truncated orders of $N = 3, 4, 5, 6$. From Figure 1, we observe that when choosing $N = 5, 6$, we already complete the task with the average value for $M_x(T)$ higher than 0.999.

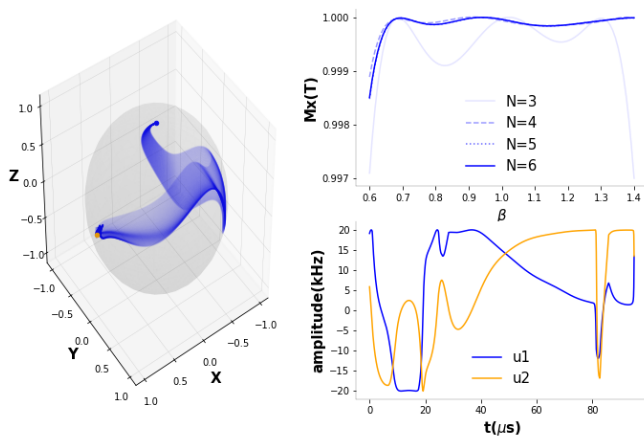

Fig. 1. Simulation results for uniform pulse design with $T = 3.8\pi$. The subfigures highlight the ensemble state trajectory on Bloch sphere (left panel), pattern of ensemble states $M_x(T, \beta)$ obtained from different truncation orders N (upper right panel), and the computed control inputs for $N = 5$ (lower right panel).

2) Uniform Inversion Pulse in the Presence of RF-inhomogeneity: An inversion pulse nutates the magnetization vector from the direction of the main magnetic field $M_0(\beta) = (0, 0, 1)'$ to its opposite pole, i.e., $M_f(\beta) = (0, 0, -1)'$. The results for this task are detailed in Figure 2, where we utilize a truncation order $N = 6$ to obtain the truncated moment dynamics, and the average value for the obtained $M_z(T)$ is -0.9997. The left figure in Figure 2 showcases sampled trajectories for the magnetization vector evolving under the obtained control input.

3) Uniform Excitation Pulse in the Presence of Larmor Dispersion and RF-inhomogeneity: In a more challenging scenario, in which Larmor dispersion and rf-inhomogeneity prevail simultaneously within the spin population, the proposed moment-based method is, once more, capable of exciting the ensemble uniformly. In this context, minor adaptations are adopted to define the corresponding moment

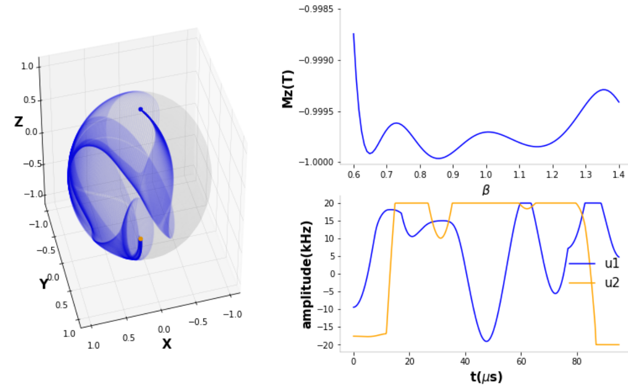

Fig. 2. Simulation results for uniform inversion pulse design using a truncation order $N = 6$ for $T = 3.8\pi$. The subfigures highlight the ensemble state trajectory (left panel), final pattern of ensemble states $M_z(T, \beta)$ (upper right panel), and the computed optimized inputs (lower right panel).

dynamics, which are detailed in Appendix B. The performance for the obtained excitation pulse is demonstrated in Figure 3, where the parameters are set as $K = 1$, $T = 4\pi$ and $N = 8$. The proposed method achieves an average value for $M_x(T)$ above 0.994.

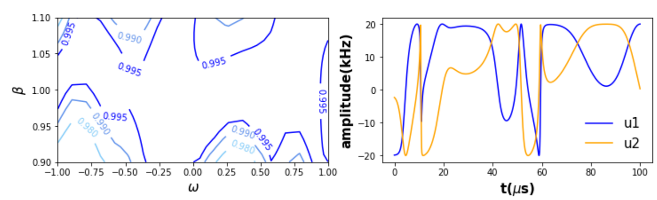

Fig. 3. Simulation result for uniform pulse design using truncated order $N = 8$ for two parameterization case.

B. Selective Excitation Pulse

Selective excitation pulses affect spins only within a specific frequency range, leaving the remaining population unaffected at the end of the pulse duration. For this application, the target state in the case of rf-inhomgeneity is specified as the following,

$$M_f(\beta) = \begin{cases} (1, 0, 0)', & 0.9 \leq \beta \leq 1.1 \\ (0, 0, 1)', & 0.6 \leq \beta < 0.9 \cup 1.1 < \beta \leq 1.4 \end{cases}$$

Notice that $M_f(\beta)$ has infinitely many nonzero moment terms, which compels the implementation of a larger truncation order in the control design via moment dynamics. However, we can simplify the computation process by subdividing this problem into three uniform pulse design problem corresponding to three different range of the parameter, i.e., $\beta \in [0.6, 0.9) \cup (1.1, 1.4]$ (the corresponding trajectories of M_x and M_z are depicted in washed blue color in Figure 4), and $\beta \in [0.9, 1.1]$ (the corresponding trajectories of M_x and M_z are in blue color in Figure 4). The results in Figure 4 are obtained by using truncation order $N = 10$ and $T = 50$. Furthermore, we perform a selective excitation pulse in the

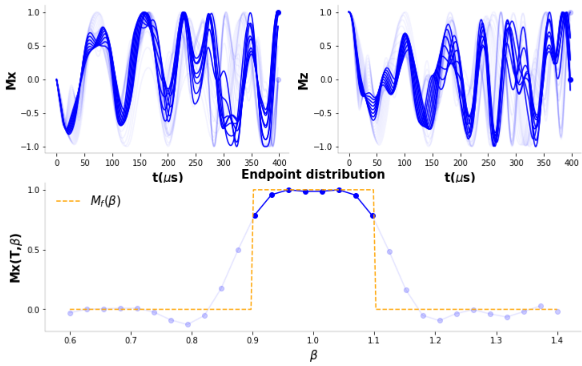

Fig. 4. Simulation result for selective excitation pulse for $T = 50$ using truncated order $N = 10$.

case of Larmor dispersion with the desired magnetization vector given as,

$$M_f(\omega) = \begin{cases} (1,0,0)', -0.2 \leq \omega \leq 0.2 \\ (0,0,1)', -1 \leq \omega < -0.2 \cup 0.2 < \omega \leq 1 \end{cases}$$

The obtained simulation result is displayed in Figure 5 where $N = 20$ and $T = 100$ are used.

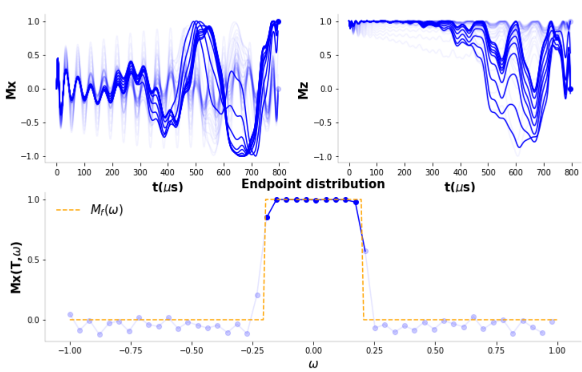

Fig. 5. Simulation result for selective pulse design for $T = 100$ using truncated order $N = 20$.

V. Conclusion

This paper devises a novel pulse design method for manipulating bulk magnetization of spin ensembles by considering the moment dynamics accompanying Bloch ensemble systems. The proposed moment-based method presents promising performance in enhancing sensitivity in NMR and MRI applications. We conduct error analysis on the truncation of infinite-dimensional moment dynamics, paving the way for constructing controls in a finite-dimensional setting, where any effective nonlinear control algorithms can be implemented. Furthermore, we have validated our approach in different scenarios of system inhomogeneity in Bloch equations by designing optimal pulses that realized uniform, selective, and inversion excitation patterns. The simplicity, yet efficacy, of the proposed approach allows it to be exploited in a wide range of applications of pulse design in quantum control and enables researchers to conduct experiments that require sophisticated pulse design scenarios.

Appendix

A. Derivation of dimensionless ensemble dynamics

The dynamics of spin ensemble in a rotation frame is described as

$$\frac{d}{dt}M = \begin{pmatrix} 0 & -\Delta\omega & \beta\frac{\Sigma(t)}{\gamma}\sin(\phi) \\ \Delta\omega & 0 & -\beta\frac{\Sigma(t)}{\gamma}\cos(\phi) \\ \beta\frac{\Sigma(t)}{\gamma}\sin(\phi) & \beta\frac{\Sigma(t)}{\gamma}\cos(\phi) & 0 \end{pmatrix} M,$$

where Σ and ϕ are the amplitude and phase of the applied rf field, and $\Delta\omega \in [-\tilde{K}, \tilde{K}]$ (unit in Hertz) denotes the variations in Larmor frequency, $\beta \in [1-\delta, 1+\delta]$ denotes the inhomogeneity in rf field, with $\tilde{K} > 0$ and $\delta \in (0,1)$. To obtain its dimensionless description as given in (1), a normalization is performed by using a nominal pulse amplitude A_0 so that we have the following correspondences, $\omega = \Delta\omega/A_0 \in [-K, K]$ with $K = \tilde{K}/A_0$; the controls are normalized as well, $u_1(t) = \frac{\gamma\Sigma(t)}{A_0}\cos(\phi(t))$, $u_2(t) = \frac{\gamma\Sigma(t)}{A_0}\sin(\phi(t))$; t in (1) denotes a dimensionless time obtained from scaling physical time by $2\pi A_0$.

B. Ensemble dynamics with different parameterization

Ω_x, Ω_y and Ω_z are generator of rotations along x, y and z axis, which are skew-symmetric specified by

$$\Omega_x = \begin{pmatrix} 0 & 0 & 0 \\ 0 & 0 & -1 \\ 0 & 1 & 0 \end{pmatrix}, \Omega_y = \begin{pmatrix} 0 & 0 & 1 \\ 0 & 0 & 0 \\ -1 & 0 & 0 \end{pmatrix}, \Omega_z = \begin{pmatrix} 0 & -1 & 0 \\ 1 & 0 & 0 \\ 0 & 0 & 0 \end{pmatrix}.$$

For Bloch ensembles with only parameterization ω (i.e. $\delta = 0$), we have that

$$\dot{M}(t,\omega) = \left(\omega A + \sum_{i=1}^{2} u_i B_i\right) M(t,\omega),$$

whose associated moment dynamics is derived by defining moment terms $m_k = \int_{-1}^{1} P_k(\omega) M(t,\omega) d\omega$,

$$\dot{m}(t) = \left(\hat{A} + \sum_{i=1}^{2} u_i \hat{B}_i\right) m(t), \tag{10}$$

where $\hat{A} = \mathcal{C}_0 \otimes A$ and $\hat{B}_i = \mathcal{I} \otimes B_i$ are bounded operators, and $\mathcal{C}_0$ and $\mathcal{I}$ are the same as given in the main text.

For a more general form of Bloch ensembles as in (2), we first define the moments by utilizing products of Legendre polynomials $\{P_k(\omega)P_l(\beta)\}$,

$$m_{k,l}(t) = \int_{-1}^{1}\int_{-1}^{1} P_k(\omega)P_l(\beta)M(t,\omega,\beta)d\beta d\omega,$$

where $m_{k,l}(t) \in \ell^2(\mathbb{R}^n) \times \ell^2(\mathbb{R}^n)$. If we consider $\omega \in [-K, K]$ and $\beta \in [1-\delta, 1+\delta]$, the dynamics of the moment terms $m_{k,l}$ are derived accordingly as

$$\dot{m}_{k,l}(t) = K\left[C_k A m_{k-1,l} + C_{k+1} A m_{k+1,l}\right] + \sum_i u_i \left[\delta C_l B_i m_{k,l-1} + \delta C_{l+1} B_i m_{k,l+1} + B_i m_{k,l}\right].$$

If truncation order of N is used, we obtain the truncated moment dynamics,

$$\dot{\bar{m}}_N(t) = \left(\hat{A}_N + \sum_{i=1}^{2} u_i \hat{B}_{Ni}\right) \bar{m}_N(t),$$

where $\bar{m}_N = (m'_{0,0}, \ldots, m'_{0,N}, m'_{1,0}, \ldots, m'_{N,N})'$, and

$$\hat{A}_N = \begin{pmatrix} \ddots & \ddots & & \\ \ddots & 0 & 1 & \\ & 1 & \ddots & \ddots \\ & & \ddots & \ddots \end{pmatrix}_{N\times N} \otimes \left(\operatorname{diag}(K\hat{C}_N) \otimes A\right),$$
$$\hat{B}_{Ni} = I \otimes (C_\delta \otimes B_i),$$

with $C_\delta = \mathcal{C}_{N\times N}$, $\hat{C}_N = (C_1, C_2, \ldots, C_N)$, and I denotes the identity matrix of matching dimension.

C. Derivation of Legendre-moment system

By the moment definition in (3), we have the kth order moment equals to $m_k(t) = \int_{-1}^{1} P_k(\beta) M(t,\beta)\,\mathrm{d}\beta$ and it is differentiable in t since $[-1,1]$ is compact. The normalized Legendre polynomials $P_0(\beta) = \frac{1}{\sqrt{2}}$, $P_1(\beta) = \sqrt{\frac{3}{2}}\beta$, $\ldots$ satisfy the following orthonormality and recurrence relations: for any $i, j \in \mathbb{N}$ and $k \in \mathbb{Z}_+$,

$$\langle P_i, P_j\rangle = \int_K P_i(\beta) P_j(\beta)\,\mathrm{d}\beta = \delta_{ij},$$
$$C_{k+1} P_{k+1}(\beta) = \beta P_k(\beta) - C_k P_{k-1}(\beta),$$

Since the set $\{P_k\}$ constitutes an orthonormal basis for $L^2([-1,1])$, and considering (3), an ensemble state $M(t,\cdot) \in L^2([-1,1])$ can be represented as a Legendre polynomial series:

$$M(t,\cdot) = \sum_{k=0}^{\infty} m_k(t) P_k(\cdot).$$

The above Legendre polynomial series consequently induces an isometric isomorphism between $M(t,\cdot) \in L^2([-1,1])$ and $m(t) \in \ell^2$.

REFERENCES

[1] A. Dupré, K.-M. Lei, P.-I. Mak, R. P. Martins, and W. K. Peng, "Micro-and nanofabrication nmr technologies for point-of-care medical applications–a review," *Microelectronic Engineering*, vol. 209, pp. 66–74, 2019.

[2] F. Aiello, J. Gerretzen, M. G. Simons, A. N. Davies, and P. Dani, "A multivariate approach to investigate the nmr cpmg pulse sequence for analysing low mw species in polymers," *Magnetic Resonance in Chemistry*, vol. 59, no. 2, pp. 172–186, 2021.

[3] A. Kosenkov, M. Gulyaev, V. Lobyshev, G. Yusubalieva, and V. Baklaushev, "The reversible effect of deuteration on tissue fluid and biopolymers in normal and tumor tissues of mice," *Biophysics*, vol. 63, no. 5, pp. 820–824, 2018.

[4] J. P. de Almeida Martins, C. M. Tax, F. Szczepankiewicz, D. K. Jones, C.-F. Westin, and D. Topgaard, "Transferring principles of solid-state and laplace nmr to the field of in vivo brain mri," *Magnetic Resonance*, vol. 1, no. 1, pp. 27–43, 2020.

[5] J. B. W. Webber, "A review of the use of simple time-domain nmr/mri for material-science," *SN Applied Sciences*, vol. 3, no. 10, pp. 1–18, 2021.

[6] J. Cavanagh, W. J. Fairbrother, A. G. Palmer III, and N. J. Skelton, *Protein NMR spectroscopy: principles and practice*. Academic press, 1996.

[7] M. A. Bernstein, K. F. King, and X. J. Zhou, *Handbook of MRI pulse sequences*. Elsevier, 2004.

[8] V. M. Runge, M. L. Wood, D. M. Kaufman, and M. S. Silver, "Mr imaging section profile optimization: improved contrast and detection of lesions.," *Radiology*, vol. 167, no. 3, pp. 831–834, 1988.

[9] M. Shinnar and J. S. Leigh, "The application of spinors to pulse synthesis and analysis," *Magnetic resonance in medicine*, vol. 12, no. 1, pp. 93–98, 1989.

[10] J. Mao, T. Mareci, K. Scott, and E. Andrew, "Selective inversion radiofrequency pulses by optimal control," *Journal of Magnetic Resonance (1969)*, vol. 70, no. 2, pp. 310–318, 1986.

[11] K. Kobzar, B. Luy, N. Khaneja, and S. J. Glaser, "Pattern pulses: design of arbitrary excitation profiles as a function of pulse amplitude and offset," *Journal of Magnetic Resonance*, vol. 173, no. 2, pp. 229–235, 2005.

[12] B. Pryor and N. Khaneja, "Fourier decompositions and pulse sequence design algorithms for nuclear magnetic resonance in inhomogeneous fields," *The Journal of chemical physics*, vol. 125, no. 19, p. 194111, 2006.

[13] J.-S. Li and N. Khaneja, "Ensemble control of bloch equations," *IEEE Transactions on Automatic Control*, vol. 54, no. 3, pp. 528–536, 2009.

[14] W. Zhang and J.-S. Li, "Uniform and selective excitations of spin ensembles with rf inhomogeneity," in *2015 54th IEEE Conference on Decision and Control (CDC)*, pp. 5766–5771, IEEE, 2015.

[15] S. Zeng and F. Allgoewer, "A moment-based approach to ensemble controllability of linear systems," *Systems & Control Letters*, vol. 98, pp. 49–56, 2016.

[16] K. Kuritz, S. Zeng, and F. Allgöwer, "Ensemble controllability of cellular oscillators," *IEEE Control Systems Letters*, vol. 3, no. 2, pp. 296–301, 2018.

[17] X. Ning, G. Cheng, and J.-S. Li, "Control design of linear ensemble via moment dynamics." 2022.

[18] R. Triggiani, "Controllability and observability in banach space with bounded operators," *SIAM Journal on Control*, vol. 13, no. 2, pp. 462–491, 1975.

[19] E. Heintze and X. Liu, "Homogeneity of infinite dimensional isoparametric submanifolds," *Annals of mathematics*, vol. 149, no. 1, pp. 149–181, 1999.

[20] M. K. Salehani and I. Markina, "Controllability on infinite-dimensional manifolds: a chow–rashevsky theorem," *Acta Applicandae Mathematicae*, vol. 134, no. 1, pp. 229–246, 2014.

[21] J.-S. Li, J. Ruths, T.-Y. Yu, H. Arthanari, and G. Wagner, "Optimal pulse design in quantum control: A unified computational method," *Proceedings of the National Academy of Sciences*, vol. 108, no. 5, pp. 1879–1884, 2011.

[22] Y. M. Berezansky, Z. G. Sheftel, and G. F. Us, *Functional analysis. Vol. I*, vol. 85 of *Operator Theory: Advances and Applications*. Birkhäuser Verlag, Basel, 1996. Translated from the 1990 Russian original by Peter V. Malyshev.

[23] Q. Gong, W. Kang, and I. M. Ross, "A pseudospectral method for the optimal control of constrained feedback linearizable systems," *IEEE Transactions on Automatic Control*, vol. 51, no. 7, pp. 1115–1129, 2006.

[24] N. Khaneja, T. Reiss, C. Kehlet, T. S.-Herbruggen, and S. J. Glaser, "Optimal control of coupled spin dynamics: design of NMR pulse sequences by gradient ascent algorithms," *Journal of Magnetic Resonance*, vol. 172, pp. 296–305, 2005.

[25] J. Ruths and J.-S. Li, "A multidimensional pseudospectral method for optimal control of quantum ensembles," *Journal of Chemical Physics*, vol. 134, p. 044128, 2011.

[26] M. Benzi and G. H. Golub, "Bounds for the entries of matrix functions with applications to preconditioning," *BIT Numerical Mathematics*, vol. 39, no. 3, pp. 417–438, 1999.

[27] M. Shao, "On the finite section method for computing exponentials of doubly-infinite skew-hermitian matrices," *Linear Algebra and its Applications*, vol. 451, pp. 65–96, 2014.

[28] S. Zeng, "Iterative optimal control syntheses illustrated on the brockett integrator," *IFAC-PapersOnLine*, vol. 52, no. 16, pp. 138–143, 2019.